BMC Musculoskeletal Disorders

RESEARCH

Open Access

A new distal radius fracture classification depending on the specific fragments through machine learning clustering method

Yuling Gao[1,4], Yanrui Zhao[1,4], Yang Liu[1,4], Shan Lei[1,4], Hanzhou Wang[1,4], Yuerong Lizhu[2,5], Tianchao Lu[1,4], Zhexian Cheng[3,6], Dong Wang[1,4], Binzhi Zhao[1,4], Ziyi Li[1,4] and Junlin Zhou[1,4*]

Abstract

Purposes The objective of this study was to investigate intra-articular distal radius fractures, aiming to provide a comprehensive analysis of fracture patterns and discuss the corresponding treatment strategies for each pattern.

Methods 294 cases of intra-articular distal radius fractures lines were collected and clustered thorough K-means and hierarchical clustering algorithm. The demographic data of patients and the clinical treatment outcomes were recorded. For functional evaluation, quick Disabilities of the Arm, Shoulder, and Hand (DASH) score, visual analog scale (VAS) pain score, range of motion (ROM) of the wrist joint and the percentage of the grip strength relative to the healthy wrist at 12 months follow-up were evaluated and recorded; For radiographic parameters of volar tilt (VT), radial inclination (RI), and ulnar variance (UV) were obtained; The occurrence of complications was carefully assessed and documented.

Results Totally 294 patients were included and divided into the volar side affected group and the dorsal side affected groups. And each group was further categorized into three types: type I, with two parts fractures with either one volar/dorsal side intact; type II, with three parts fractures with volar/dorsal side simply affected; and type III, with four parts fractures with volar/dorsal side communited affected. The volar plate fixation was performed as the standard treatment, while the combined plate fixation was used for comminuted dorsal bone defects of the metaphysis and impaction. There were no differences in the postoperative radiograph parameters, functional outcomes and incidences of complications for each type of volar side group and dorsal side group except that the 3.2 type DRFs showed less range of flexion (75.56±7.48)° and extension (61.65±9.9)° than other dorsal types.

Conclusions A new intra-articular distal radius fractures classification was proposed based on the affection condition of volar or dorsal side. The volar plate fixation is an effective treatment for the intra-articular distal radius fractures, while combined plate fixation can be considered as an alternative treatment for dorsal side comminuted fractures.

Level of evidence III a

Keywords Distal radius fractures, Articular, Specific fragment, Machine learning, Classification, Plate fixation, Combined fixation

*Correspondence:
Junlin Zhou
junlinzhou_article@outlook.com
Full list of author information is available at the end of the article

Introduction

The distal radius fracture (DRF) is one of the most common fracture types representing 16% of all [1]. Intra-articular fractures are common in DRFs representing approximately 60% of all DRFs, which are caused by a complex interplay of various forces such as tension on ligament, bone compression and shearing forces [2, 3]. Drawing upon CT scans and three-dimensional (3D) reconstructions, surgeons can gain a deeper understanding of the fracture patterns. The surgical intervention is necessary for intra-articular fractures to achieve proper anatomical reconstruction of the articular surface and ensure secure fixation. It was discovered that the presence of ligament insertions could lead to recurring fracture lines especially in many two-part fractures and the term "osteoligamentary unit" was introduced [4, 5]. According to the biomechanical functions and anatomical characteristics, the articular fragments were identified and termed. Based on the three column theory, fragments at the intermediate column include volar rim, dorsal ulnar corner (DUC), dorsal wall, and free intra-articular fragments [6]. The utilization of specific fragment fixation in the clinical management of DRFs has been proposed as an efficacious treatment for several years [6–8].

However, there also exist the controversy in the concept of the specific fragment fixation. On the one hand, the current literature lacks a comprehensive and systematic description of the distribution of intra-articular fracture lines in DRFs, resulting in an unclear understanding of the fracture pattern. On the other hand, a contentious debate also exists regarding the optimal treatment for intra-articular DRFs, specifically between volar treatment and alternative treatments. The meaching learning method provided an opportunity to analysis amount complex fracture lines. Li, Jiantao et al. [9] collected 504 intertrochanteric fractures of preoperative CT data and focused on a clustering analysis of morphological fracture lines to identify classifications. In this study, we aimed to study 294 intra-articular DRFs to summarize the fracture patterns and discuss the treatment for each pattern of fractures.

Methods

Patients and fractures modeling

Between January 2016 and December 2022, 426 consecutive patients diagnosed with distal radius fractures were recruited retrospectively at the department of orthopedics of the local hospital. The inclusion criteria were listed as below: (1) intra-articular fracture of distal radius; (2) patient aged 18 years or older; and (3) preoperative CT scans with the slice thickness below 1.5 mm). We excluded patients according to the following: (1) previous surgery on the affected wrist; (2) mental disorders; (3) open fractures; (4) fractures with associated neurovascular injuries; and (5) old fractures. The demographic information of the patients was documented, encompassing numerical data, gender distribution, injury side specification, AO/OTA (Arbeitsgemeinschaft für Osteosynthesefragen /Orthopaedic Trauma Association) classification and dislocation side identification. The fracture-dislocation of the radiocarpal joint is distinguished by a lack of connection between the carpus and distal radius which can be further classified into volar dislocation, dorsal dislocation, and neutral dislocation [10].

Each patient data from CT scans were exported in data Digital Imaging and Communications in Medicine (DICOM) format to the Mimics 21.0 system (Materialise, Belgium) where the 3D segments were reconstructed and the fractures were simultaneously reduced. And then the fracture model was imported into 3-maticresearch 13.0 (Materialise, Belgium) software. Through Adobe Photoshop CC 2015 (Adobe Systems Software Ireland, Dublin, Ireland), the intro-articular fracture lines were extracted and recorded. Each intra-articular fracture line could be recorded and translated as a matrix through the Python code (img filename list, img color = cv.imread, img resize = cv.resize, img gray = cv.cvtColor, img bin = cv.threshold, img bin). And then we need to calculate its distance to all other data points, using the Hausdorff distance method to effectively illustrate the variations among cases due to discrepancies in the total pixel count on fracture lines. The formula of Hausdorff distance can be expressed as $h(A, B) = \max(a \in A)\{ \min(b \in B) \{ d(a - b) \}\}$.

The K-means method and the Hierarchical clustering were common clustering methods in the medical fields [11]. The K-means method is a clustering based classification algorithm, which works by iteratively updating the cluster centers such that the distance between each cluster center and all sample points is minimized [12]. The procedure was performed as follows: 1.The initial clustering centers were randomly selected from K data points. 2.Data points were reassigned to the nearest cluster center based on distance calculations, which may require multiple iterations until each point is correctly assigned. 3.New cluster centers were determined by calculating the mean of all data points within each cluster. The Hierarchical clustering is a method that systematically groups data using either a top-down or bottom-up approach, known as divisive and agglomerative hierarchical clustering respectively [13]. The Hausdorff distance is used to calculate the distances between all data points and create a distance matrix. Then, a hierarchical clustering algorithm is applied using this matrix for clustering. A

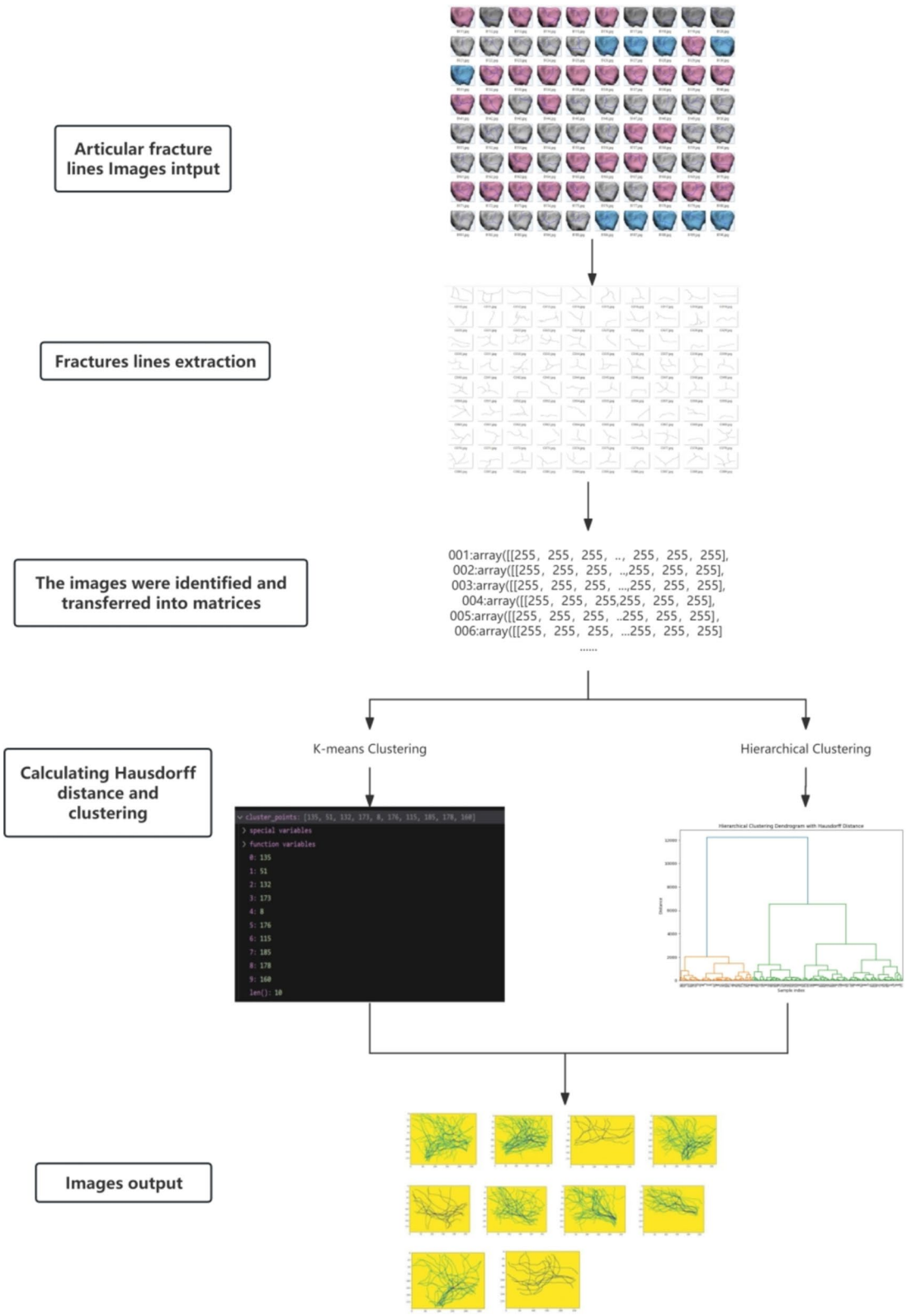

Fig. 1 The flowchart of machine learning procedure on the DRFs

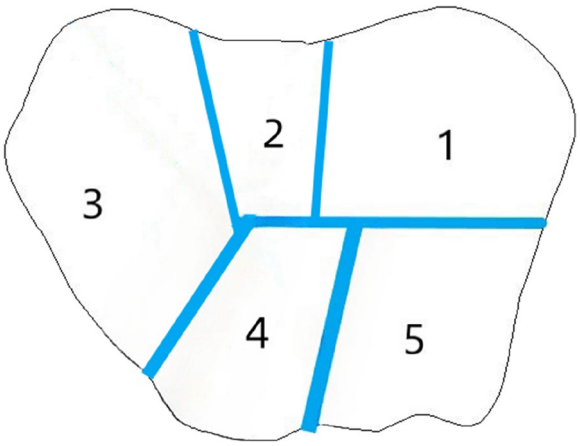

Fig. 2 The definition of the fragment in distal radius fractures: 1.the volar rim fragment, 2. the intermediate fragment, 3. the radial styloid fragment, 4. the dorsal wall fragment, 5. the dorsal ulnar corner(DUC) fragment; 4 + 5: the dorsal rim fragment

flowchart was made to describe the procedure of applying this method to DRFs as seen at Fig. 1.

As our experience on the knowledge of DRFs morphology, we categorized the intra- articular affected degree into three types: two fragments parts fractures, three fragments parts fractures and over three parts fragments fractures.The images produced by machine learning methods were numbered and voted by six experienced trauma surgeons. After a week, the image acquisition procedure was repeated, and subsequently, inter-observer and intra-observer reliability were assessed using the kappa statistic.

Fragments identification

The distal radius can be divided into three columns based on the biomechanical view: radial column, intermediate column and ulnar column [14]. Accordingly, we identified based on the three column model.The location of fragments at the articular surface can be seen at Fig. 2.

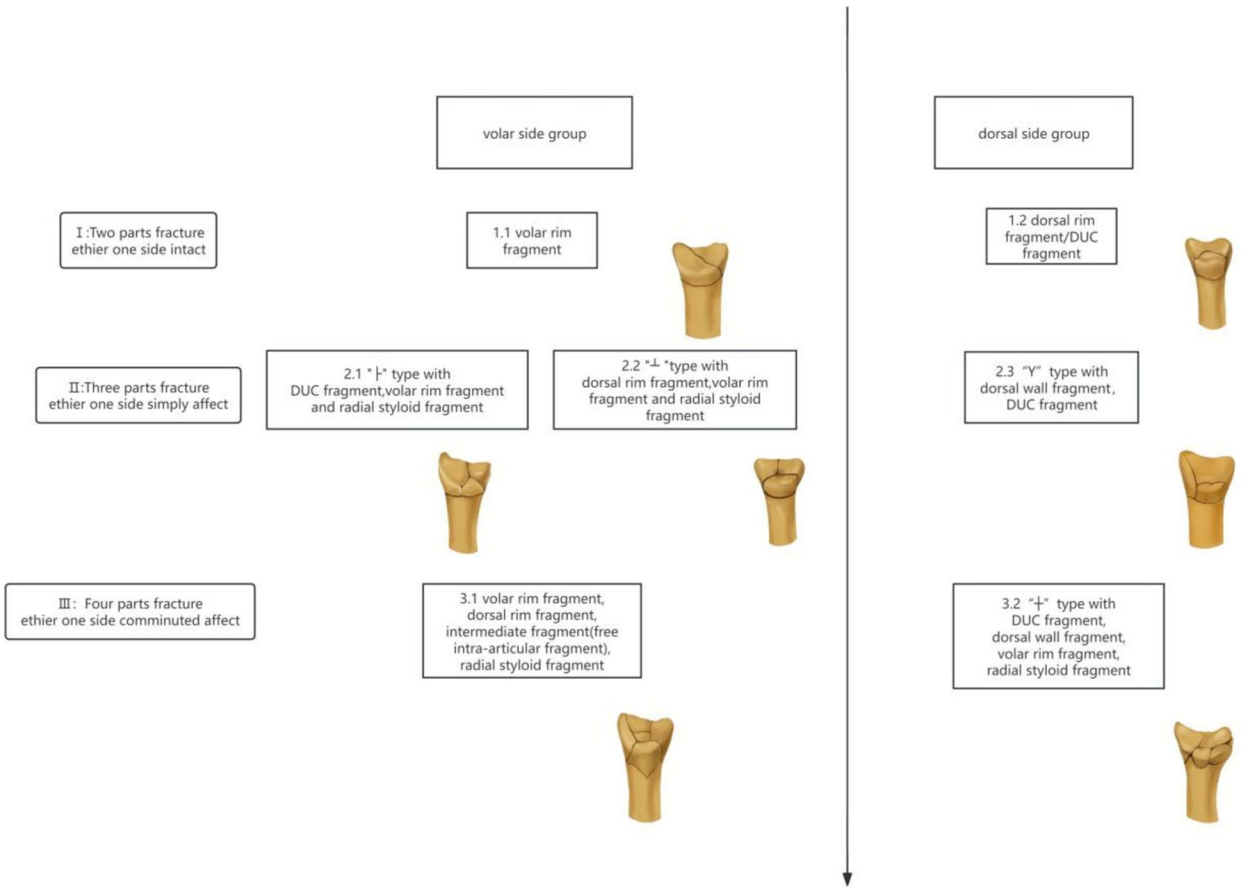

Fig. 3 The intra-articular DRFs were grouped into 2 groups depending on side affected and 3 types depending on the side affected degree. Each group was further categorized into three types: type I, with two parts fractures with either one volar/dorsal side intact; type II, with three parts fractures with volar/dorsal side simply affected; and type III, with four parts fractures with volar/dorsal side communited affected

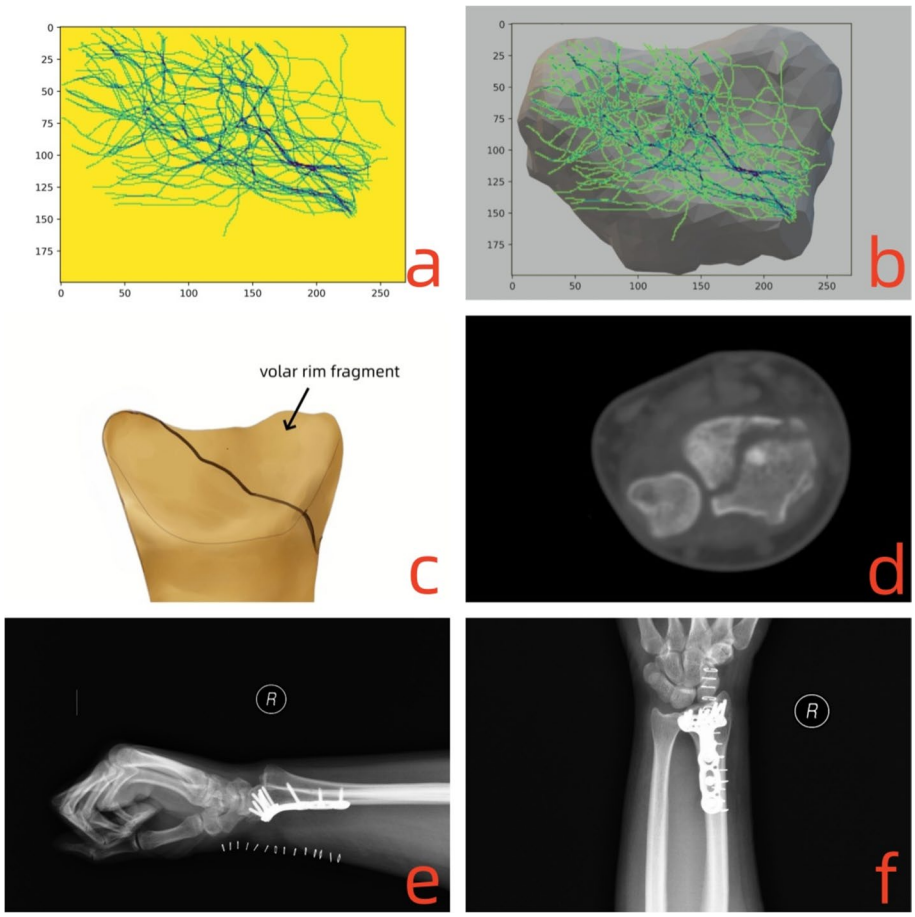

Fig. 4 For type 1.1 DRFs, the fracture line traversed from the the sigmoid notch to the volar side articular surface. The morphological characteristics and the clinical treatment were shown as follows: **a**)-**b**) the fracture lines clustered by and covered on the intra-articular surface; **c**) the model for type 1.1 DRFs; **d**) the CT scan for the fracture lines at the articular surface; **e**)-**f**) postoperative posteroanterior and lateral X-ray images

The radial styloid fragments mainly include the radial column structure with the brachioradialis tendon and the radioscaphocapitate and long radiolunate ligaments inserted.

The volar rim fragments are formed by the flat volar surface of the distal radius containing the fossa of lunate with short and long radiolunate ligaments inserted. In our study, the fragments distributed between the radial styloid fragments and the volar rim fragments are named the intermediate fragments. The impacted articular pieces caused by higher energy violence are named the intra-articular fragments [7].

The dorsal rim fragments as a a footprint for the origin of the dorsal radiocarpal ligament are formed by the thin cortex and irregular dorsal side surface including the dorsal wall fragments and the DUC fragments. The characteristic anatomic landmark of dorsal wall fragments mainly include the Lister notch. And the DUC fragments mainly include the dorsal corner of the distal radioulnar joint constituting the bony rim of the sigmoid notch and serving as the origin of the dorsal radioulnar ligaments [15]. One of the most important ligaments inserted at the DUC fragments is the triangular fibrocartilage complex as an important stabilizer of the distal radioulnar joint [16].

Postoperative evaluation

For functional evaluation, quick Disabilities of the Arm, Shoulder, and Hand (DASH) score, visual analog scale (VAS) pain score, range of motion (ROM) of the wrist joint and the percentage of the grip strength relative to the healthy wrist at 12 months follow-up were evaluated and recorded; For radiographic evaluation relevant measurements of volar tilt (VT), radial inclination (RI), and ulnar variance (UV) were obtained using standard immediate postoperative posteroanterior and lateral

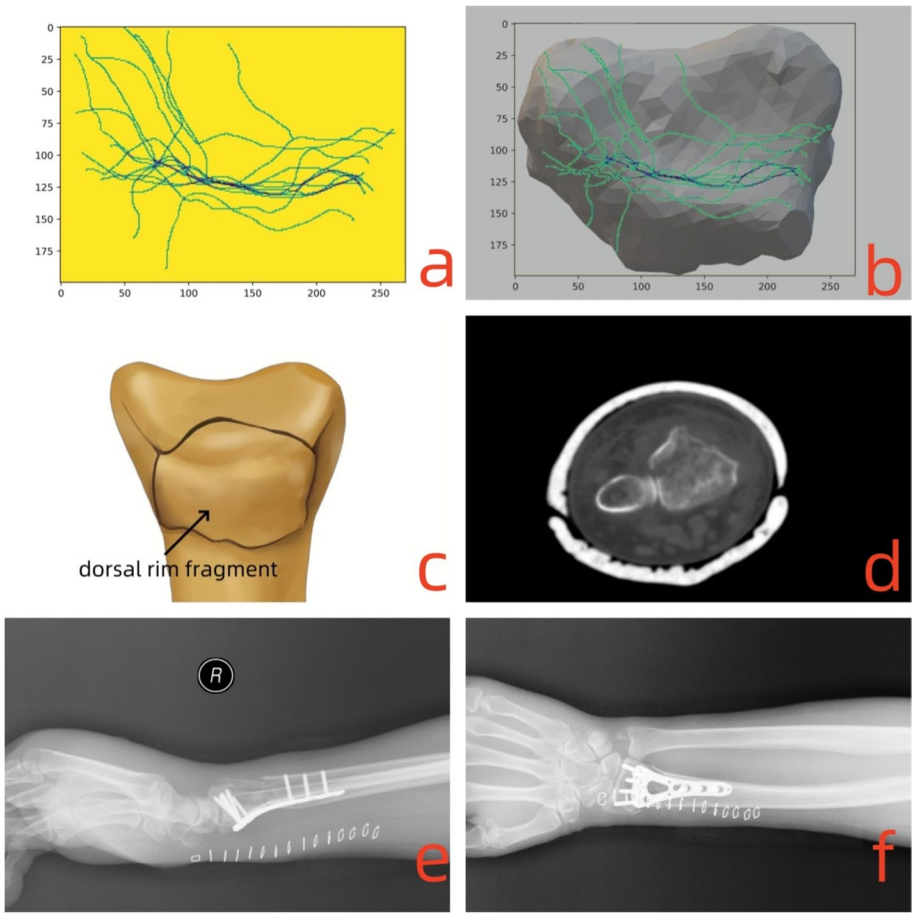

Fig. 5 For type 1.2 DRFs, the coronal fracture line is closed to the dorsal side and forms the dorsal fragment. The morphological characteristics and the clinical treatment were shown as follows: a)-b) the fracture lines clustered and covered on the intra-articular surface; c) the model for type 1.2 DRFs; d) the CT scan for the fracture lines at the articular surface; e)-f) postoperative posteroanterior and lateral X-ray images

radiographs; The occurrence of complications was carefully assessed and documented during each follow-up period, encompassing reduction loss, infection, nerve injury, tendon injury, irritation related to internal fixation and removal of implant. This section of the study involved the participation of six experienced surgeons, who were responsible for both implementing the methodology and validating the collected data.

Table 1 Patients demographic data in type I

	1.1	1.2	*p*
Number, n	60	30	
Age, year	55.5 ± 15.6	59 ± 20.9	0.059
Gender(male: female), n	18:42	8:22	0.447
Injuried side(left: right), n	26:34	12:18	0.231
AO classification, n			
(B3:C1:C2:C3)	32:20:6:2	2:22:3:3	0.021*
Dislocation side, n			
(volar direction: dorsal direction: neutral direction)	57:0:3	10:8:12	<0.001*

*$p<0.05$

Surgical technique

Most patients were applied for the volar plate fixation for the standard treatment. The patients were placed in a supine position under a local or general anesthesia. A incision about 6 cm was made through the Henry approach. The fragments were fixed with the volar plate under the fluoroscopic guidance. Either autogenous bone graft or allograft was utilized for the purpose of filling the bone defect. For difficult reduced dorsal fragments or impacted intra-articular fragments, the method of volar plating with limited dorsal open reduction was applied. Typically, a 4–5 cm incision is made on the dorsal side above the Lister tubercle in the dorsal approach. The extensor retinaculum is divided in a Z-shaped manner, and after subperiosteal dissection, the fracture is exposed through the fourth extensor compartment. Reduction of impacted articular fragments takes place. The dorsal plate

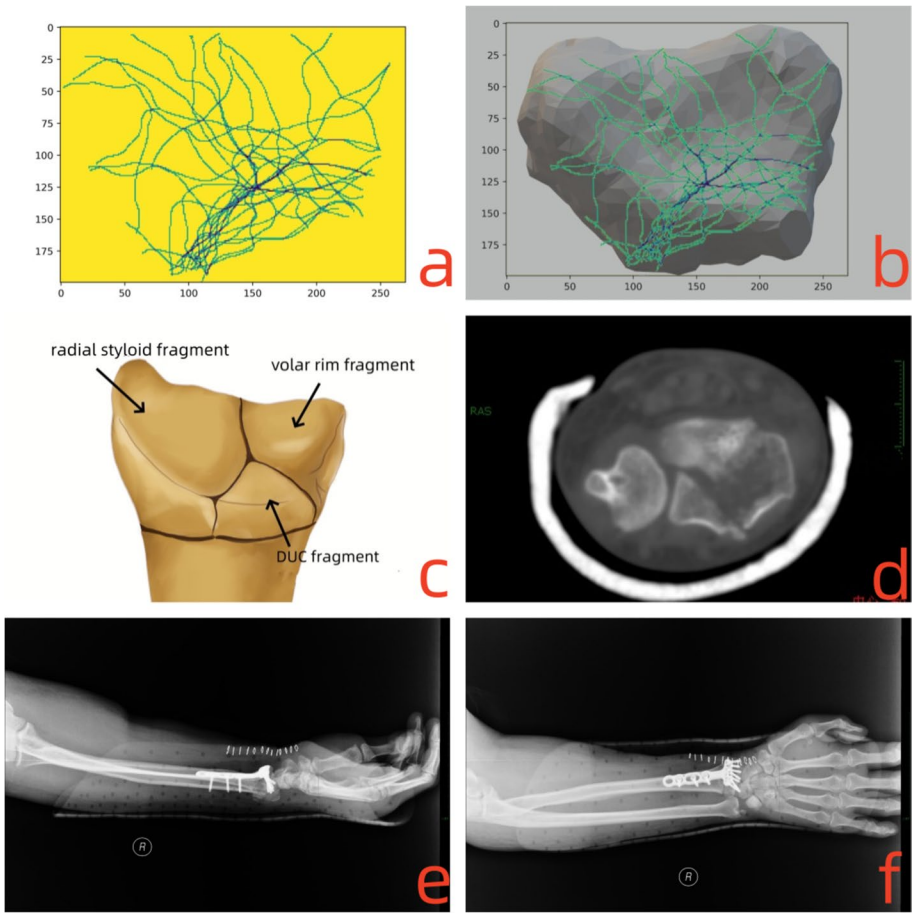

Fig. 6 For type 2.1 DRFs, the fracture lines originated from the sigmoid notch and extended to the dorsal and volar side of the articular surface forming a distinctive "├" shape. The morphological characteristics and the clinical treatment were shown as follows: **a**)-**b**) the fracture lines clustered and covered on the intra-articular surface; **c**) the model for type 2.1 DRFs; **d**) the CT scan for the fracture lines at the articular surface; **e**)-**f**) postoperative posteroanterior and lateral X-ray images

is fixed using screws from proximal to distal direction, with the plate serving as a reduction tool. The combined plate fixation method was used for severe impaction of the dorsal cortex with bone defects in the metaphysis.

After the surgery, a cast was used to immobilize the affected area for 4 weeks in cases of comminuted fractures. The cast and auxiliary K-wires were removed after approximately 1 month, followed by gradual commencement of active and passive wrist rehabilitation.

Statistical analysis

Statistical analysis was performed using SPSS version 22.0 (SPSS Inc, Chicago, Illinois, USA). Landis and Koch's [17] standards were used to interpret the statistical results: the closer the Kappa value is to 1, the better the correlation; the smaller the Kappa value, the worse the correlation. Values > 0.80 reflect almost perfect agreement; 0.61–0.80 indicate substantial agreement; 0.41–0.60 suggest moderate agreement; 0.21–0.40 imply fair agreement; and values between 0 and 0.20 represent slight agreement. Continuous variables data was conducted by using single sample K–S test and run test to test the normal distribution. Independent sample non-parametric test or independent sample t test and Kendall's concordance coefficient were used according to whether the distribution was normal. And the ANVOA(analysis of variance) test was used for the comparison with more than 2 groups. Chi-square test was used for dichotomous variables. A p-value < 0.05 was considered statistically significant.

Results

Totally 294 patients were included and divided into the volar side affected group and the dorsal side affected groups. And each group was further categorized into three types: The Type I was defined as fractures consisting of two parts, with either the volar or dorsal side

intact. It included two subtypes with an inter-observer reliability of 0.73 and an intra-observer reliability of 0.85; The type II was defined as three parts fractures with volar/dorsal side simply affected. It included three subtypes with an inter-observer reliability of 0.69 and an intra-observer reliability of 0.89; The type III was defined as four parts fractures with volar/dorsal side communited affected. It included two subtypes with an inter-observer reliability of 0.80 and an intra-observer reliability of 0.84. The details could be seen in Fig. 3.

Type I DRFs include 69 volar side affected patients for type 1.1 and 30 dorsal side affected patients for type 1.2. The characteristics of Type I DRFs included intact volar rim fragments in type 1.1 as shown in Fig. 4, and intact DUC fragments or dorsal rim fragments in type 1.2 as depicted in Fig. 5. There was significant difference between type 1.1 (B3:C1:C2:C3, 32:20:6:2) and type 1.2 (B3:C1:C2:C3, 2:22:3:3) DRFs in the distribution of the AO classification ($p=0.021$). The majority of the type 1.1 dislocation direction concentrate on the volar direction with 57 cases, while the type 2.2 had 10 volar direction fractures, 8 dorsal direction and 12 neutral direction. The different direction cases between two groups distribution showed significant difference ($p<0.001$). The details of patients demographic data could be seen in Table 1.

Type II DRFs were characteristic for three parts fractures with volar/dorsal side simply affected. The articular fracture lines divide the articular surface into three parts. In the volar side group of type II DRFs ($n=69$), The morphological characteristics of type 2.1 DRFs and Type 2.2 DRFs can be seen in Figs. 6 and 7. In the dorsal side group, 35 cases of type 2.3 DRFs were characterized like "Y" shape as shown in Fig. 8. The details of patients demographic data could be seen in Table 2.

Type III DRFs with either one side comminuted fractured included 58 volar side affected patients for type 3.1 and 42 dorsal side affected patients for type 3.2. The morphological characteristics of comminuted volar side

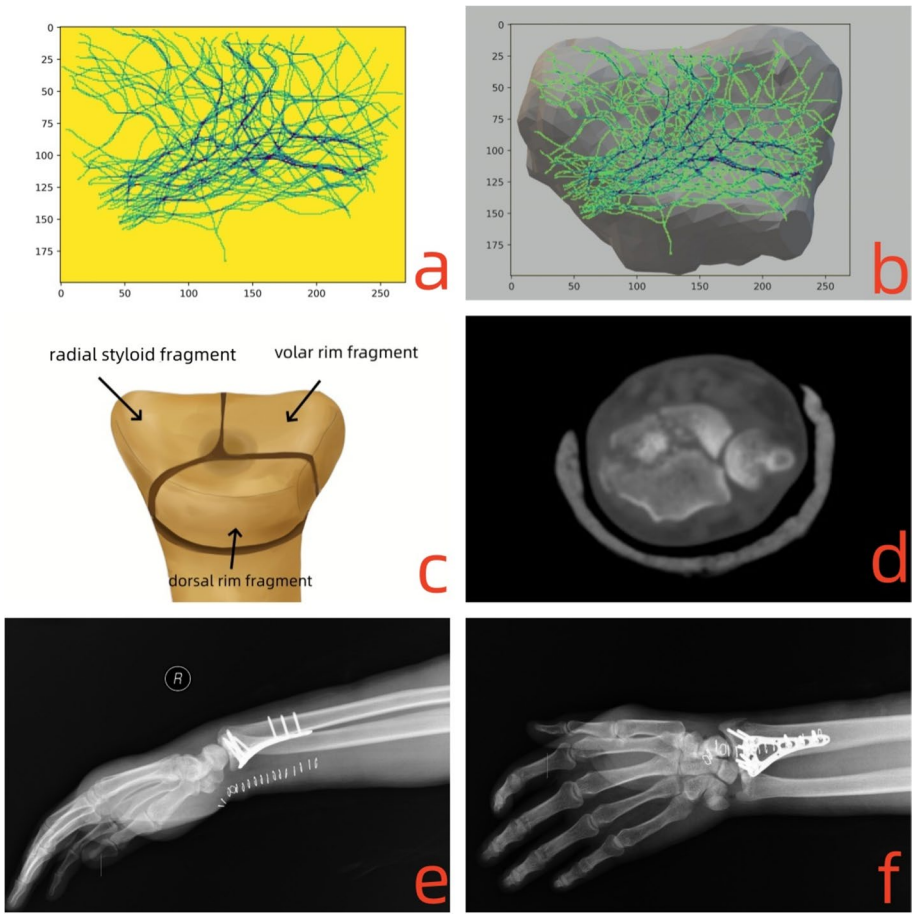

Fig. 7 For type 2.2 DRFs, the fracture lines traversed coronally through the articular surface and extended to the volar side like "⊥" shape. The morphological characteristics and the clinical treatment were shown as follows: **a**)-**b**) the fracture lines clustered and covered on the intra-articular surface; **c**) the model for type 2.2 DRFs; **d**) the CT scan for the fracture lines at the articular surface; **e**)-**f**) postoperative posteroanterior and lateral X-ray images

in type 3.1 DRFs and comminuted dorsal side in type 3.2 can be seen in Figs. 9 and 10. There was significant difference between type 3.1 (B3:C3.1:C3.2:C3.3, 20:19:16:3) and type 3.2 (B3:C3.1:C3.2:C3.3, 5:8:27:2) DRFs in the distribution of the AO classification ($p=0.008$). The dislocation direction of type 3.1 DRFs includes 52 cases in the volar direction, 3 cases in the dorsal direction, and 3 cases in the neutral direction. For type 3.2 DRFs, there are 30 cases in the dorsal direction, 4 cases in the volar direction, and 8 cases in the neutral direction. There was a significant difference between these two types regarding dislocation directions ($p<0.001$). The details of patients demographic data could be seen in Table 3.

As shown in the Table 4, there were no differences in the postoperative radiograph parameter, range of motion, the functional outcome and the incidences of complications for each type of volar side group.

As shown in the Table 5, there were no differences in the postoperative radiograph parameter, the functional outcome and the incidences of complications for each type of dorsal side group. The 3.2 type DRFs showed less range of flexion (75.56 ± 7.48°) and extension (61.65 ± 9.9°) than other dorsal types ($p<0.05$).

Discussion

Fracture mapping technology combined with CT scan technology have been applied for revealing the fracture lines characteristic of the intra-articular DRFs [18–20]. For the current classifications of DRFs, the AO/OTA classification is the most widely used and comprehensive classification. The Fernandez classification focused on the mechanism of injury. However, both of them lack further description of the articular fractures affected situation. A few classifications, such as the Mayo classification for the lunate fossa and sigmoid fossa affected situation, and the Melone classification for the intermediate column affected situation, describe types of intra-articular DRFs. But the current classifications of intra-articular DRFs are limited to describing the affected area of the

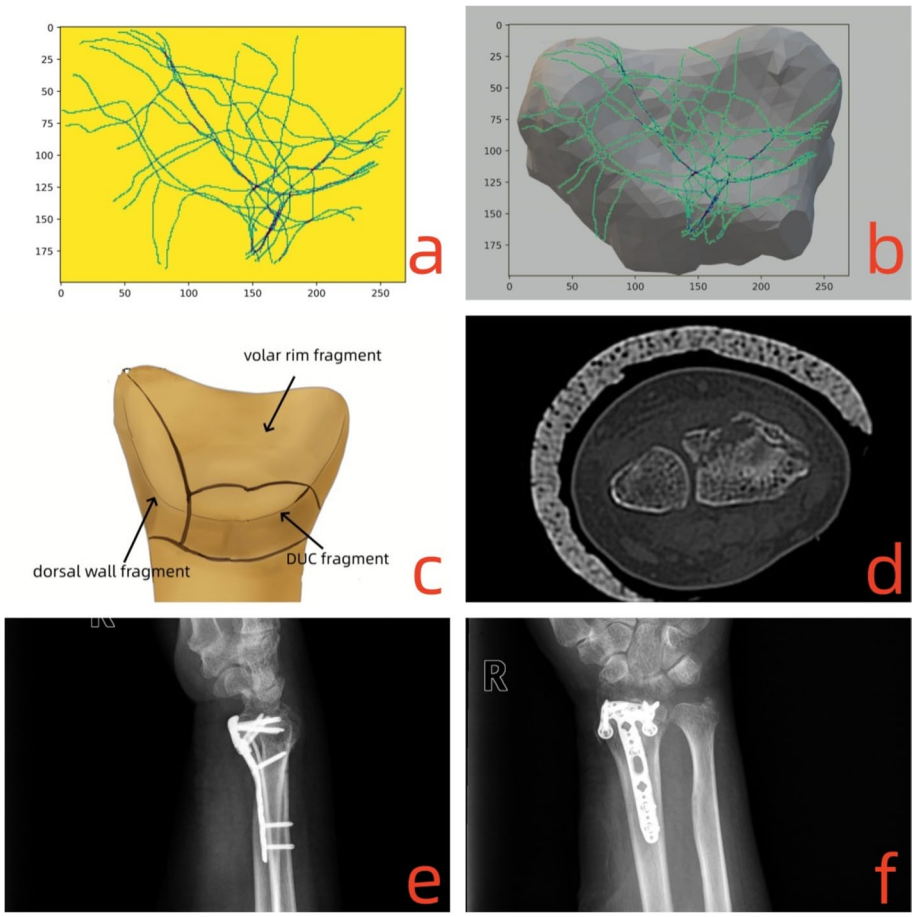

Fig. 8 For type 2.3 DRFs, the fracture lines traversed along the dorsal side and radial styloid forming like "Y" shape. The morphological characteristics and the clinical treatment were shown as follows: **a**)-**b**) the fracture lines clustered and covered on the intra-articular surface; **c**) the model for type 2.3 DRFs; **d**) the CT scan for the fracture lines at the articular surface; **e**)-**f**) postoperative posteroanterior and lateral X-ray images

Table 2 Patients demographic data in type II

	2.1 + 2.2	2.3	*p*
Number, n	69	35	
Age, year	50 ± 14.9	56.5 ± 22.0	0.866
Gender(male: female), n	31:38	17:18	0.993
Injuried side(left: right), n	36:33	13:22	0.237
AO classification, n			
(B3:C3.1:C3.2:C3.3)	12:8:1:48	0:7:8:20	0.069
Dislocation side, n			
(volar direction: dorsal direction: neutral direction)	33:7:29	7:5:23	0.212

fracture, lacking specific descriptions of the fracture lines and fragments, thus having limited impact on clinical guidance and the development of surgical treatment strategies. Our study stepped further to distinguish different fracture lines types from complex intra-articular fracture lines through machine learning methods. To the best of our knowledge, it is the first study trying to identified and classified intra-articular DRFs according to the specific fragments and distal radius articular sides of fracture lines affected. The surgeons could gain a better understanding of the patterns of intra-articular DRFs, enabling them to choose between regular volar plate fixation or other fixation strategies.

For unstable DRFs, it were defined by Orbay and Fernandez with radiographic evidence of 15°angle at least on orthogonal plane as well as an articular step or possible radius shortening bigger than 2 mm [21]. In our study, the dislocation direction was mainly formed by the volar side dislocation. But compared to the volar side affected group, the dorsal side dislocation incidences were relative higher than the volar side affected group. And most of the dorsal side dislocation belonged to the subluxation apart from the 3.2 type DRFs. For volar side affected group, we suspected that the violence force are mainly caused by the impaction force concentrating on the volar side with

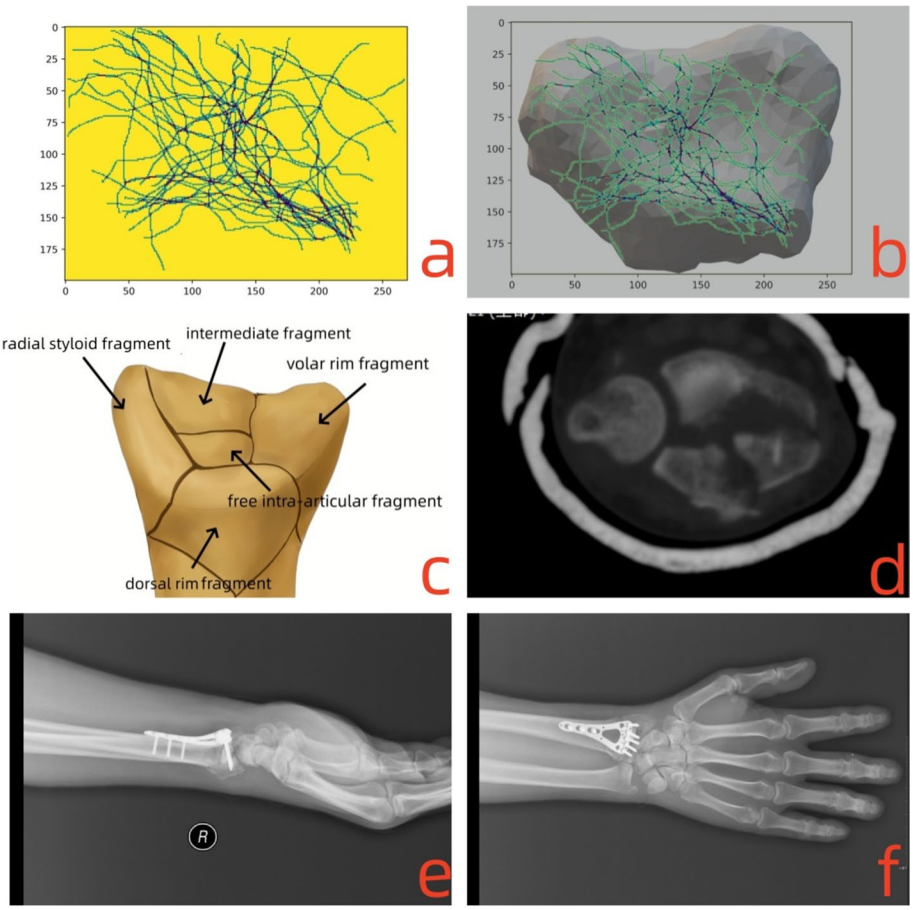

Fig. 9 For type 3.1 DRFs, the fracture lines derived from the sigmoid notch, dorsal side, radial side and volar side, and crossed along the interfossal ridge forming like "×" shape. The morphological characteristics and the clinical treatment were shown as follows: **a**)-**b**) the fracture lines clustered and covered on the intra-articular surface; **c**) the model for type 3.1 DRFs; **d**) the CT scan for the fracture lines at the articular surface; **e**)-**f**) postoperative posteroanterior and lateral X-ray images

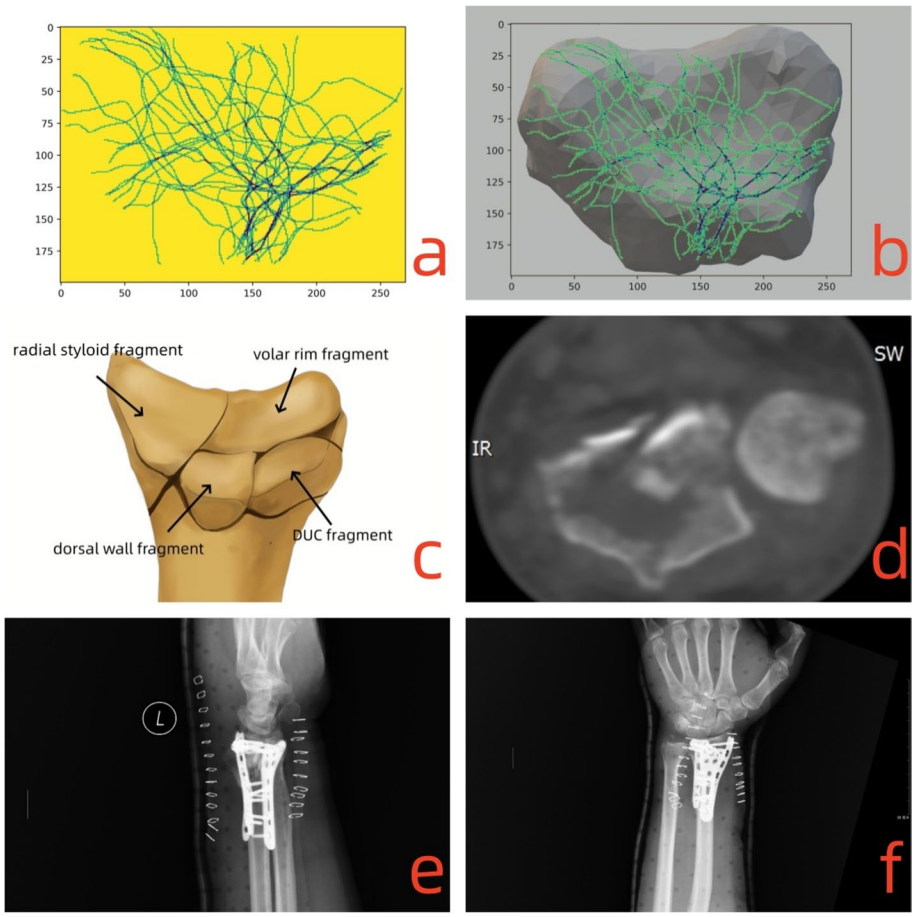

Fig. 10 For type 3.2 DRFs, the fracture lines derived from the sigmoid notch, dorsal side, radial side and volar side, and crossed along the interfossal ridge forming like "+" shape. The morphological characteristics and the clinical treatment were shown as follows: **a**)-**b**) the fracture lines clustered and covered on the intra-articular surface; **c**) the model for type 3.2 DRFs; **d**) the CT scan for the fracture lines at the articular surface; **e**)-**f**) postoperative posteroanterior and lateral X-ray images

or without the dorsal side affected. Therefore the B type of AO classification fractures could exist in any subtype DRFs in the volar side affected group.

The dorsal part of DRFs were studied in previous study focusing on the dorsal cortex and the dorsal dislocation [10, 22–24]. Our study showed that the dorsal fragments usually indicated the complete articular fracture (type C fracture in the AO classification). Souer JS also supported that the volar shearing fractures were usually complete articular fracture (75%) and the identification of dorsal cortex fracture would avoid the inadequate dorsal plate or percutaneous fixation [22]. Daly MC depicted the fragment number of dorsal cortical breaks ranging from 2 to 4 pieces [25]. Biondi M divided the dorsal dislocation DRFs into three groups which the dorsal types depicted in our study are in accordance with [10]. The comminuted metaphyseal and depression fractures usually affected around the dorsal wall fragment. The dorsal dislocation in DRFs is largely due to the dorsal articular surface impaction and the avulsion of the radiocarpal ligaments.

In our volar side affected group, the VLP fixation has achieved satisfying outcome and no differences were found in the assessment of functional scores and radiographic parameters. Similarly, other studies have showed the VLP fixation as an effective treatment for the volar Barton's fractures and C type fractures [26, 27]. No differences of radiographic parameters and functional scores assessments were found in the volar side affected group, which could be accounted by that the improved anatomic parameters provided by the VLP fixation for the advantage of clear vision and room for the implant [28].

For dorsal side affected group, the volar approach increase the difficulty of the capture for dorsal rim fragments, although the volar plate fixation has the advantage of the sufficient room and the flat cortex for implant placement [29, 30]. Zimmer J showed that the use of screws that extend only 75% across the distal

Table 3 Patients demographic data in type III

	3.1	3.2	*p*
Number, n	58	42	
Age, year	52.14 ± 13.93	56.76 ± 12.29	0.23
Gender(male: female), n	32:26	19:23	0.194
Injuried side(left: right), n	34:24	20:22	0.3
AO classification, n			
(B3:C3.1:C3.2:C3.3)	20:19:16:3	5:8:27:2	0.008*
Dislocation side, n			
(volar direction: dorsal direction: neutral direction)	52:3:3	4:30:8	<0.001*

*$p<0.05$

radius would generally not capture the DUC fragment [31]. The treatment for the dorsal fragment is still be controversial. Type 3.2 DRF is formed by volar rim fragment, radial styloid fragment, dorsal wall fragment and DUC fragment and involves dorsal side severely comminuted. The die-punch fragment firstly defined as the dorso-medial fragments separated from the lunate facet particularly represents a great challenge for surgical treatment [32]. Due to restoring anatomical alignment and articular congruity is essential for satisfactory functional result, we take combined plating fixation for the treatment of DRFs with bone defects of the metaphysis and significant impaction of the dorsal wall fragments. For dorsal severely comminuted DRFs as well as four-part DRFs, the combined plate fixation are proposed to be effective to reconstruct the functional wrist [26, 27]. In a retrospective cohort study, Rozental and Blazar also found similar DASH scores between dorsal plates group and volar group despite that the volar plates group increased the risk of loss of reduction and malunion [33]. However compared to the volar plate fixation, the combined plating fixation may have a negative effect on wrist ROM and that hard ware removal is more frequently need in patients treated with combined plating [28, 34]. In our study, the type 3.2 DRFs showed less range of flexion and extension than other dorsal types. Although no statistically significant differences were observed in complication rates among the various dorsal groups, it appears that the incidences of internal fixation irritation and implant removal are comparatively higher than those associated with other dorsal types. Similarly, Biondi M divided the dorsal fracture-dislocation into four types and the type IV with large dorsal wall fragments and volar side both affected also showed less favourable outcomes [10]. The phenomenon could be accounted for that dorsal plating might lead to the displacement of the reduced fragment in cases of severe dorsal comminution and induce extensor tendon irritation [28, 35].

There are several limitations in our study. Firstly, though each type was clustered through the machine learning method, the identification and selection from several types provided by the machine learning still depended on the subjective simplification. Secondly, because of multiple planes provided by the CT scan,

Table 4 The treatment outcome in the volar affected group

	1.1	2.1	2.2	3.1
Postoperative radiograph parameter				
VT	13.77 ± 5.01	10.15 ± 5.70	12.27 ± 4.80	13.09 ± 4.89
RI	19.95 ± 4.17	20.02 ± 4.12	21.51 ± 3.97	21.67 ± 4.41
UV	−0.04 ± 0.15	−0.02 ± 0.40	−0.13 ± 0.09	0.13 ± 0.16
Range of motion				
Flexion°	78.17 ± 6.6	80.06 ± 3.20	84.25 ± 6.98	81.56 ± 7.48
Extension°	65.29 ± 7.5	58.41 ± 16.3	57.68 ± 23.6	61.65 ± 9.9
Supination°	92.48 ± 6.2	84.61 ± 14.3	88.15 ± 11.6	86.70 ± 15.4
Pronation°	89.65 ± 13.9	92.02 ± 15.6	87.57 ± 8.4	86.36 ± 20.3
Functional score				
DASH score	4.4 ± 3.1	3.7 ± 2.0	5.5 ± 2.8	4.2 ± 3.4
VAS score	0.7 ± 0.2	1.1 ± 0.7	1.9 ± 1.1	1.7 ± 0.6
Grip strength	82.63 ± 2.5%	83.11 ± 10.5%	79.18 ± 7.8%	80.89 ± 5.9%
Complication				
Infection	0	2	1	1
Reduction loss	0	0	1	2
Nerve injury	1	0	0	1
Irritation of internal fixation	4	1	3	3
Tendon injury	1	0	1	0
Removal of implant	6	7	9	7

Table 5 The treatment outcome in the dorsal affected group

	2.2	2.3	3.2
Postoperative radiograph parameter			
VT	13.30 ± 4.35	10.76 ± 3.20	12.27 ± 2.53
RI	22.02 ± 5.00	22.94 ± 4.66	24.022 ± 3.43
UV	−0.09 ± 0.20	0.15 ± 0.251	0.02 ± 0.25
Range of motion			
Flexion°	79.17 ± 6.6	80.06 ± 3.20	75.56 ± 7.48[a]
Extension°	68.29 ± 7.5	72.41 ± 16.3	61.65 ± 9.9[b]
Supination°	92.48 ± 6.2	84.61 ± 14.3	86.70 ± 15.4
Pronation°	89.65 ± 13.9	92.02 ± 15.6	86.36 ± 20.3
Functional score			
DASH score	4.7 ± 0.8	5.1 ± 1.2	5.9 ± 1.3
VAS scroe	0.5 ± 0.2	1.6 ± 1.0	1.4 ± 0.3
Grip strength	88 ± 5.9%	89 ± 3.3%	86 ± 8.5%
Complication			
Infection	0	1	1
Reduction loss	2	0	2
Nerve injury	0	0	0
Irritation of internal fixation	0	2	12
Tendon injury	0	0	0
Removal of implant	4	5	17

[a] the flexion degree in the 3.2 group exhibited significant differences compared to the 2.2 group ($p = 0.02$), as well as compared to the 2.3 group ($p = 0.04$)

[b] the extension degree in the 3.2 group exhibited significant differences compared to the 2.2 group ($p = 0.008$), as well as compared to the 2.3 group ($p = 0.01$)

there may exist errors in selecting distal radius articular plane which may take the metaphysis fractures mistake for articular fractures. The limited number of surgeons (six in total) with expertise and technique may introduce potential bias, thereby influencing outcomes and reducing external validity. The reliance on CT-based 3D reconstruction limits the applicability of the findings to settings without readily available imaging. Studies that consider the influence of different surgical techniques and surgeon expertise would offer a more nuanced understanding of treatment outcomes. Thirdly, though 294 patients were enrolled in our study, there still can involved patients as many as possible in the machine learning method. Apart from increasing the sample size, external datasets would also validate the classification's applicability. Meanwhile, the lack of diversity in patient backgrounds needs to be addressed to improve the study's relevance across different clinical settings. At last but not least, due to the optimal treatment for intra-articular DRFs is still controversy, the comparisons of functional outcomes across different treatment methods need to be further debate. The focus of our study lies in proposing various fracture pattern morphologies, while lacking the evidence necessary to address treatment choices.

Conclusion

A new intra-articular distal radius fractures classification was proposed based on the affection condition of volar or dorsal side. The volar plate fixation is an effective treatment for the intra-articular distal radius fractures, while combined plate fixation can be considered as an alternative treatment for dorsal side comminuted fractures.

Acknowledgements
We thank Kai Yan for providing programming support.

Authors' contributions
All listed authors have contributed substantially to this work: Yuling Gao: Wrote the original draft of the manuscript and performed the methodology. Yanrui Zhao: Performed the operation and provided the patients data Lei Shan: Performed the operation and provided the patients data Hanzhou Wang: Design the methodology of machine learning method Yuerong Lizhu: Provided the radiological imaging data and performed the measurement of the postoperative parameters Tianchao Lu: Performed the made and revision of the new classification Zhexian Cheng: Design the methodology of machine learning method Dong Wang: Performed the operation and provided the patients data Binzhi Zhao:Performed the statistic part and the made and revision of the new classification Ziyi Li:Performed the made and revision of the new classification Yang Liu: designed and revised the whole procedure of the study Junlin Zhou: Acquired the funding and in charge of this study.

Funding
The correspondence author Junlin Zhou discloses receipt of the following financial support for the research, authorship, and publication of this article: National Natural Science Foundation of China (82272469) and Beijing Key Clinical Specialty Project.

Data availability
The datasets used and/or analysed during the current study are available from the corresponding author on reasonable request.

Declarations

Ethics approval and consent to participate
This study was approved by the Ethics Committee of Chaoyang Hospital, Capital Medical University in accordance with the Declaration of Helsinki.(Clinical trial number :2021-科-441;Registration Date: 2021/7/5) Informed consent to participate was obtained from all of the participants in the study.

Consent for publication
Not applicable.

Competing interests
The authors declare no competing interests.

Author details
[1]Orthopedics Department, Affiliated Beijing Chaoyang Hospital of Capital Medical University, Bejing, China. [2]Rediology, Affiliated Beijing Tiantan Hospital of Capital Medical University, Beijing, China. [3]Preventive Dentistry Department, Affiliated Stomatology Hospital of Guangzhou Medical University, Guangzhou, Guangdong Province, China. [4]Beijing Chaoyang Hospital, Capital Medical University, Gongtinan Road 8#, Beijing 100020, China. [5]Beijing Tiantan hospital, Capital Medical University, Fanyang Road 115#, Beijing 100050, China. [6]Affiliated Stomatology Hospital of Guangzhou Medical University, Dongfeng Road(West)Yuexiu District 195#, Guangzhou 511495, China.

Received: 13 September 2024 Accepted: 18 December 2024
Published online: 30 December 2024

References

1. Constant CR, Gerber C, Emery RJ, Søjbjerg JO, Gohlke F, Boileau P. A review of the constant score: modifications and guidelines for its use. J Shoulder Elb Surg. 2008;17(2):355–61. https://doi.org/10.1016/j.jse.2007.06.022.
2. Cooney WP 3rd, Linscheid RL, Dobyns JH. External pin fixation for unstable Colles' fractures. J Bone Joint Surg Am. 1979;61(6A):840–5.
3. Leung KS, Shen WY, Tsang HK, Chiu KH, Leung PC, Hung LK. An effective treatment of comminuted fractures of the distal radius. J Hand Surg Am. 1990;15(1):11–7. https://doi.org/10.1016/s0363-5023(09)91098-x.
4. Mandziak DG, Watts AC, Bain GI. Ligament contribution to patterns of articular fractures of the distal radius. J Hand Surg Am. 2011;36(10):1621–5. https://doi.org/10.1016/j.jhsa.2011.07.014.
5. Bain GI, Alexander JJ, Eng K, Durrant A, Zumstein MA. Ligament origins are preserved in distal radial intraarticular two-part fractures: a computed tomography-based study. J Wrist Surg. 2013;2(3):255–62. https://doi.org/10.1055/s-0033-1355440.
6. Rhee PC, Medoff RJ, Shin AY. Complex distal Radius fractures: an anatomic algorithm for Surgical Management. J Am Acad Orthop Surg. 2017;25(2):77–88. https://doi.org/10.5435/JAAOS-D-15-00525.
7. Hozack BA, Tosti RJ. Fragment-specific fixation in distal radius fractures. Curr Rev Musculoskelet Med. 2019;12(2):190–7. https://doi.org/10.1007/s12178-019-09538-6.
8. Pulos N, Shin AY. Strategies for specific reduction in high-energy distal Radius fractures. Hand Clin. 2021;37(2):267–78. https://doi.org/10.1016/j.hcl.2021.02.009.
9. Li J, Tang S, Zhang H, Li Z, Deng W, Zhao C, Fan L, Wang G, Liu J, Yin P, Xu G, Zhang L, Tang P. Clustering of morphological fracture lines for identifying intertrochanteric fracture classification with Hausdorff distance-based K-means approach. Injury. 2019;50(4):939–49. https://doi.org/10.1016/j.injury.2019.03.032.
10. Biondi M, Lauri G. Dorsal fracture-dislocation of the radiocarpal joint: a new classification and implications in surgical treatment. J Hand Surg Eur. 2020;45(7):700–8. https://doi.org/10.1177/1753193420926801.
11. Werner E, Clark JN, Hepburn A, Bhamber RS, Ambler M, Bourdeaux CP, et al. Explainable hierarchical clustering for patient subtyping and risk prediction. Exp Biol Med (Maywood). 2023;248(24):2547–59. https://doi.org/10.1177/15353702231214253.
12. Jain AK. Data clustering: 50 years beyond K-means. Pattern Recogn Lett. 2009;31:651–66.
13. McLachlan GJ, Bean RW, Ng SK. Clustering Methods Mol Biol. 2017;1526:345–62. https://doi.org/10.1007/978-1-4939-6613-4_19.
14. Rikli DA, Regazzoni P, Babst R. Die dorsale Doppelplattenosteosynthese am distalen Radius–ein biomechanisches Konzept und dessen klinische Realisation [Dorsal double plating for fractures of the distal radius–a biomechanical concept and clinical experience]. Zentralbl Chir. 2003;128(12):1003–7. https://doi.org/10.1055/s-2003-44839. German.
15. Lamas C, Llusà M, Méndez A, Proubasta I, Carrera A, Forcada P. Intraosseous vascularity of the distal radius: anatomy and clinical implications in distal radius fractures. Hand (N Y). 2009;4(4):418–23. https://doi.org/10.1007/s11552-009-9204-9.
16. Jupiter JB. Complex articular fractures of the distal Radius: classification and management. J Am Acad Orthop Surg. 1997;5(3):119–29. https://doi.org/10.5435/00124635-199705000-00001.
17. Landis JR, Koch GG. The measurement of observer agreement for categorical data. Biometrics. 1977;33(1):159–74.
18. Misir A, Ozturk K, Kizkapan TB, Yildiz KI, Gur V, Sevencan A. Fracture lines and comminution zones in OTA/AO type 23C3 distal radius fractures: the distal radius map. J Orthop Surg (Hong Kong). 2018;26(1):2309499017754107. https://doi.org/10.1177/2309499017754107.
19. Zhang X, Zhang Y, Fan J, Yuan F, Tang Q, Xian CJ. Analyses of fracture line distribution in intra-articular distal radius fractures. Radiol Med. 2019;124(7):613–9. https://doi.org/10.1007/s11547-019-01025-9.
20. Li S, Zhang YQ, Wang GH, Li K, Wang J, Ni M. Melone's concept revisited in comminuted distal radius fractures: the three-dimensional CT mapping. J Orthop Surg Res. 2020;15(1):222. https://doi.org/10.1186/s13018-020-01739-x.
21. Orbay JL, Fernandez DL. Volar fixation for dorsally displaced fractures of the distal radius: a preliminary report. J Hand Surg. 2002;27(2):205–15. https://doi.org/10.1053/jhsu.2002.32081.
22. Daly MC, Horst TA, Mudgal CS. Dorsal cortical breaks in volar barton distal radius fractures. Hand (N Y). 2021;16(3):303–9. https://doi.org/10.1177/1558944719862644.
23. Lozano-Calderón SA, Doornberg J, Ring D. Fractures of the dorsal articular margin of the distal part of the radius with dorsal radiocarpal subluxation. J Bone Joint Surg Am. 2006;88(7):1486–93. https://doi.org/10.2106/JBJS.E.00930.
24. Dumontier C, Meyer zu Reckendorf G, Sautet A, Lenoble E, Saffar P, Allieu Y. Radiocarpal dislocations: classification and proposal for treatment. A review of twenty-seven cases. J Bone Joint Surg Am. 2001;83(2):212–8. https://doi.org/10.2106/00004623-200102000-00008.
25. Souer JS, Ring D, Jupiter JB, Matschke S, Audige L, Marent-Huber M, AOCID Prospective ORIF Distal Radius Study Group. Comparison of AO Type-B and Type-C volar shearing fractures of the distal part of the radius. J Bone Joint Surg Am. 2009;91(11):2605–11. https://doi.org/10.2106/JBJS.H.01479.
26. Kibar B. Combined palmar and dorsal plating of four-part distal radius fractures: our clinical and radiological results. Jt Dis Relat Surg. 2021;32(1):59–66. https://doi.org/10.5606/ehc.2021.75599.
27. Ring D, Prommersberger K, Jupiter JB. Combined dorsal and volar plate fixation of complex fractures of the distal part of the radius. J Bone Joint Surg Am. 2004;86(8):1646–52. https://doi.org/10.2106/00004623-200408000-00007.
28. Lundqvist E, Fischer P, Wretenberg P, Pettersson K, Lopez Personat A, Sagerfors M. Volar locking plate compared with combined plating of AO Type C Distal Radius fractures: a randomized controlled study of 150 cases. J Hand Surg Am. 2022;47(9):813–22. https://doi.org/10.1016/j.jhsa.2022.04.018.
29. Wong KK, Chan KW, Kwok TK, Mak KH. Volar fixation of dorsally displaced distal radial fracture using locking compression plate. J Orthop Surg (Hong Kong). 2005;13(2):153–7. https://doi.org/10.1177/230949900501300208.
30. Othman AY. Fixation of dorsally displaced distal radius fractures with volar plate. J Trauma. 2009;66(5):1416–20. https://doi.org/10.1097/TA.0b013e31817db10a.
31. Zimmer J, Atwood DN, Lovy AJ, Bridgeman J, Shin AY, Brogan DM. Characterization of the dorsal Ulnar Corner in Distal Radius fractures in Postmenopausal females: implications for Surgical decision making. J Hand Surg Am. 2020;45(6):495–502. https://doi.org/10.1016/j.jhsa.2020.02.002.
32. Yu L, Zhang X, Zhang B, Hu C, Yu K, Tian D, et al. Outcomes of volar locking plate (VLP) fixation for treatment of die-punch fracture of the distal radius: a retrospective single-surgeon study. Med (Baltim). 2019;98(33):e16796. https://doi.org/10.1097/MD.0000000000016796.
33. Rozental TD, Blazar PE. Functional outcome and complications after volar plating for dorsally displaced, unstable fractures of the distal radius. J Hand Surg Am. 2006;31(3):359–65. https://doi.org/10.1016/j.jhsa.2005.10.010.
34. Karlsson E, Wretenberg P, Björling P, Sagerfors M. Combined volar and dorsal plating vs. volar plating of distal radius fractures. A single-center study of 105 cases. Hand Surg Rehabil. 2020;39(6):516–21. https://doi.org/10.1016/j.hansur.2020.07.006.
35. Lee JH, Ahn JT, Baek JH. Dorsal plating versus volar plating with limited dorsal open reduction in the management of AO type C3 distal radius fractures with impacted articular fragments: a retrospective comparative study. Acta Orthop Traumatol Turc. 2022;56(1):42–7. https://doi.org/10.5152/j.aott.2022.21157.

Publisher's note